

Myomegalin is necessary for the formation of centrosomal and Golgi-derived microtubules

Régine Roubin^{1,2,3,4}, Claire Acquaviva^{1,2,3,4}, Véronique Chevrier^{1,2,3,4}, Fatima Sedjai^{1,2,3,4}, Déborah Zyss⁵, Daniel Birnbaum^{1,2,3,4} and Olivier Rosnet^{1,2,3,4,*}

¹Centre de Recherche en Cancérologie de Marseille, INSERM UMR1068, F-13009 Marseille, France

²Institut Paoli-Calmettes, F-13009 Marseille, France

³CNRS U7258, F-13009 Marseille, France

⁴Aix-Marseille Université, F-13007 Marseille, France

⁵Cancer Research UK Cambridge Research Institute, Li Ka Shing Centre, Cambridge CB2 0RE, UK

*Author for correspondence (olivier.rosnet@inserm.fr)

Biology Open 2, 238–250

doi: 10.1242/bio.20123392

Received 18th October 2012

Accepted 21st November 2012

Summary

The generation of cellular microtubules is initiated at specific sites such as the centrosome and the Golgi apparatus that contain nucleation complexes rich in γ -tubulin. The microtubule growing plus-ends are stabilized by plus-end tracking proteins (+TIPs), mainly EB1 and associated proteins. Myomegalin was identified as a centrosome/Golgi protein associated with cyclic nucleotide phosphodiesterase. We show here that Myomegalin exists as several isoforms. We characterize two of them. One isoform, CM-MMG, harbors a conserved domain (CM1), recently described as a nucleation activator, and is related to a family of γ -tubulin binding proteins, which includes *Drosophila* centrosomin. It localizes at the centrosome and at the *cis*-Golgi in an AKAP450-dependent manner. It recruits γ -tubulin nucleating complexes and promotes microtubule nucleation. The second isoform, EB-MMG, is devoid of CM1 domain and has a unique N-terminus with potential EB1-binding sites. It localizes at the

cis-Golgi and can localize to microtubule plus-ends. EB-MMG binds EB1 and affects its loading on microtubules and microtubule growth. Depletion of Myomegalin by small interfering RNA delays microtubule growth from the centrosome and Golgi apparatus, and decreases directional migration of RPE1 cells. In conclusion, the *Myomegalin* gene encodes different isoforms that regulate microtubules. At least two of these have different roles, demonstrating a previously unknown mechanism to control microtubules in vertebrate cells.

© 2012. Published by The Company of Biologists Ltd. This is an Open Access article distributed under the terms of the Creative Commons Attribution Non-Commercial Share Alike License (<http://creativecommons.org/licenses/by-nc-sa/3.0>).

Key words: Centrosome, EB1, Golgi, Microtubule, γ -Tubulin

Introduction

The interphase microtubule (MT) cytoskeleton regulates cell morphology and motility, organelle transport and localization, and vesicular trafficking. Nascent MTs are formed from nucleation centers containing γ -tubulin ring complexes (γ -TuRCs). Subsequently, MTs grow by tubulin dimer polymerization at their plus-end (Kollman et al., 2011). The latter process is tightly regulated and requires plus-end stabilization by interacting proteins, the best characterized being end-binding (EB) proteins, mainly EB1 (Akhmanova and Steinmetz, 2008). The major MT nucleation center in vertebrate cells is the centrosome, also known as MTOC (microtubule organizing center), but other organelles such as the nucleus and the Golgi apparatus (GA) can concentrate MT-nucleating activities at their surface (Bartolini and Gundersen, 2006; Bornens, 2002; Chabin-Brion et al., 2001). The function of MTs is strongly linked to their capacity to bridge different cellular compartments at their minus- and plus-ends, such as the centrosome and the cell cortex, to organize directional movements and cell polarity.

In many eucaryotes, proteins related to *Drosophila* centrosomin bind and regulate subcellular localization of γ -tubulin, the major

component of γ -TuRCs (Fong et al., 2008; Sawin et al., 2004; Zekert et al., 2010; Zhang and Megraw, 2007). Centrosomin regulates the recruitment of γ -tubulin to mitotic centrosomes, the formation of astral MTs and the proper orientation of mitotic spindles (Megraw et al., 2001). In fission yeast, Pcp1 and Mto1P are related proteins with similar functions that recruit γ -tubulin to spindle pole body (the equivalent of the centrosome in yeast) and non-spindle pole body associated MTOCs, respectively (Samejima et al., 2008; Sawin et al., 2004; Venkatram et al., 2004). In this protein family, *Aspergillus nidulans* AspB (Zekert et al., 2010) and mammalian CDK5RAP2/CEP215 (Fong et al., 2008) also associate with γ -tubulin to promote MT nucleation from cytoplasmic sites and centrosomes, respectively. All these proteins are large coiled-coil proteins with a small (around 60 amino acids long) N-terminal conserved domain known as the centrosomin motif 1 (CM1) (Samejima et al., 2008; Zhang and Megraw, 2007). Interestingly, the CM1 domain in centrosomin is required for γ -tubulin, D-TACC and Msps recruitment to centrosomes, but not of other centrosomal proteins such as Aurora-A and Map60 (Zhang and Megraw, 2007). In addition, a recent study has demonstrated that the CM1 domain of

CDK5RAP2 is able to bind γ -TuRCs and enhance its ability to nucleate MTs (Choi et al., 2010). This motif was therefore named γ -TuNA (γ -TuRC-mediated nucleation activator).

Myomegalin/PDE4DIP is a CDK5RAP2 paralog in vertebrates. *Myomegalin* is highly expressed in muscle tissue and its product has been described as an interactor of phosphodiesterase 4D, an enzyme controlling cAMP level (Taskén et al., 2001; Verde et al., 2001). In some mammalian cells, Myomegalin localizes to both the GA and the centrosome (Verde et al., 2001), but its function is currently unknown. Other proteins, such as CAP350 and AKAP450 (also known as AKAP9 or CG-NAP) localize at the centrosome and GA. CAP350 participates in MT anchoring at the centrosome and may stabilize MTs in the GA area to maintain its pericentrosomal structure (Hoppeler-Lebel et al., 2007). AKAP450, a γ -tubulin-interacting protein, in addition to its role as a kinase-anchoring scaffold protein at the centrosome, is also important for MT nucleation from the centrosome and GA, and for GA assembly (Hurtado et al., 2011; Takahashi et al., 1999; Takahashi et al., 2002). The GA and the centrosome cooperate in different cellular processes such as cell polarity, cell migration and ciliogenesis (Bisel et al., 2008; Follit et al., 2006; Hurtado et al., 2011; Magdalena et al., 2003; Marie et al., 2009; Sütterlin and Colanzi, 2010). Interestingly, activation of CDC42 at the GA regulates centrosome organization and function, and depends on the GA matrix protein GM130 (Kodani et al., 2009; Kodani and Sütterlin, 2008). Another GA matrix protein, GRASP65, also regulate centrosomes during mitosis (Sütterlin et al., 2005). In addition to the centrosome, the GA can be a potent MT-organizing organelle (Chabin-Brion et al., 2001; Efimov et al., 2007). Centrosome and GA-derived MTs cooperate for different functions such as proper ribbon formation and polarization during GA assembly (Vinogradova et al., 2012). The molecular machinery underlying the ability of the GA to organize MTs has begun to be identified (Efimov et al., 2007; Hurtado et al., 2011; Kim et al., 2007; Rivero et al., 2009). It includes AKAP450 and CLASP, a MT plus-end binding protein. AKAP450 is recruited to *cis*-Golgi membranes via GM130, and CLASP is anchored to the *trans*-Golgi membranes via GCC185.

In this study, we show that Myomegalin is a centrosome and *cis*-Golgi protein required for MT growth from the centrosome and GA. We also show that Myomegalin exists as several isoforms that participate by different means in MT regulation. We describe the role of two of them. The first isoform, CM-MMG, regulates MT nucleation via an interaction with the γ -TuRCs. The second isoform, EB-MMG, regulates MT dynamics via an interaction with the plus-end tracking protein (+TIP) EB1.

Materials and Methods

Cells, antibodies and reagents

Immortalized human retinal pigment epithelial cells htert-RPE1 (thereafter referred as RPE1) were grown in DMEM/F12 (Life Technologies) supplemented with 10% fetal calf serum (heat inactivated 30 minutes at 56°C).

A rabbit polyclonal antibody (Ab#1) against Myomegalin was raised against the fragment 322–939 of clone IMAGE n° 4813248, fused to GST. The fusion protein was injected in rabbits and the serum was depleted in anti-GST immunoglobulins by affinity column. The specificity of this antibody was assessed by immunofluorescence (IF) and Western blotting (Fig. 1; supplementary material Fig. S1).

Rabbit polyclonal antibody against Myomegalin (HPA008162, denoted Ab#3 in this study) was from Sigma and mouse monoclonal antibody against Myomegalin was from Abnova (M01, clone 2B5, denoted Ab#2 in this study). For Golgi compartment identification, GM130 antibody was from Abcam (rabbit monoclonal) or from BD Transduction Laboratories (mouse monoclonal),

TGN46 from AbD serotec (sheep polyclonal). MTs were stained with a rat monoclonal YL1/2 antibody (Abcam). Anti-EB1 antibodies were from BD Transduction Laboratories (mouse monoclonal), and Santa Cruz Biotech (rat monoclonal). Anti- γ -tubulin antibodies were from Sigma–Aldrich (mouse monoclonal GTU-88 and rabbit polyclonal T3559). Anti-GCP2 and NEDD1 were from Sigma–Aldrich and Novus Biological, respectively. Rabbit and mouse anti-AKAP450 were from Bethyl Laboratories and BD Biosciences, respectively. Mouse anti-c-Myc (9E10) was from Santa Cruz Biotechnology. Anti-GFP antibodies were purchased from Abcam (rabbit polyclonal) and Roche (mouse monoclonal).

Treatments

For MT depolymerisation and/or Golgi dispersal, nocodazole (10 μ M) or BFA (brefeldin-A) (5 μ g/ml) was added to the culture medium for 2 hours. For dynein inhibition experiments, cells were transfected with a myc-p50 dynamitin coding expression plasmid.

Plasmids

Full-length Myomegalin cDNAs (KIAA0477/EB-MMG and KIAA0454/CM-MMG) were obtained from the Kazusa DNA Research Institute. The sequence coding for the full-length and truncated proteins were amplified by PCR with Gateway compatible primers using Platinum HiFi polymerase (Invitrogen) and transferred into pDONR/ZEO by Gateway® recombination. The sequences were subsequently transferred by Gateway® recombination into modified Gateway-compatible pRK5-Myc, pEGFP-C1 and pmCherry-C1 expression vectors. A pcDNA3/ γ -tubulin coding vector was a gift from Alexey Khodjakov (Wadsworth Center, Albany, NY).

Cell transfection

For plasmids, cells were transfected with Fugene6 (Roche Applied Science) according to manufacturer's protocol.

Single siRNA oligonucleotides or different combinations of mixed siRNA oligonucleotides against *Myomegalin* were transfected into cells using Oligofectamin (Life Technologies) according to the manufacturer's protocol. The sequences are the following: siRNA#1 (5'-CUAACGAGCUGGAGAAUA-3'), siRNA#2 (5'-GAAGGGAAUAGUAAACUUA-3'), siRNA#3 (5'-AGA-GCGAGAUCAUGACUUA-3'), siRNA#5 (5'-CAAGAAGAAUUGCAGAAUA-3'), siRNA#7 (5'-AGAGGAAGCCCUUGGAGAA-3'). In all the experiments, a second transfection was performed at 48 hours and experiments were conducted 72 hours after the first transfection. This protocol gave the best reduction of protein expression. To deplete GM130 or AKAP450 we used a mixture of two siRNA. The sequences are as described previously (Rivero et al., 2009). To deplete EB1 we used siRNA (5'-UUGCCUUGAAGAAAGUGAA-3'). A non-targeting siRNA or siRNA targeting GAPDH were used for controls. All siRNA were purchased from Dharmacon.

Immunofluorescence

Cells were grown on coverslips, fixed in cold methanol (6–8 minutes at -20°C), saturated for 30 minutes in PBS 3% BSA and incubated with the appropriate mixture of primary antibodies for 60 minutes at room temperature. After washing in PBS 0.1% tween, they were incubated for another hour with the adequate secondary antibodies conjugated to cy2, cy3 or cy5 (Jackson laboratories) to which was added 1 μ g/ml DAPI for DNA staining, rinsed and mounted in Prolong Gold anti-fade reagent (Life Technologies). Confocal images were acquired by capturing Z-series with 0.3 μ m step size on a Zeiss LSM 510 laser scanning confocal microscope.

MT regrowth assay

RPE1 cells were cultivated on coverslips and treated with appropriate siRNA for 72 hours before the addition of 1 μ g/ml of nocodazole to the medium for 2 hours at 37°C followed by a 30-minute incubation on ice to depolymerize MTs. For repolymerization, coverslips were washed with medium and incubated 1, 3 or 5 minutes in warm medium. Before fixation, cells were permeabilized for 15 seconds in PHEM (60 mM PIPES, 25 mM HEPES, 10 mM EGTA, 4 mM MgSO₄, pH 7.0) with 0.25% Triton and 320 mM sucrose. One volume of cold methanol was added and left for an additional 45 seconds before transferring cells to pure cold methanol for 4 minutes on ice. IF was then done as usual.

EB1 dynamics

For time-lapse imaging, RPE1 EB1-GFP stable transfected cells were placed in 35 mm glass based dishes (Iwaki) and transfected as previously described with plasmid encoding mCherry-EB-MMG or mCherry-CM-MMG for 24 hours. Microscopy was carried out using a Zeiss LSM 510 laser scanning confocal microscope with a 63 \times oil lens. Images were taken every 2 seconds over 400-second periods. To determine EB1 velocity MT ends were tracked using the "track points" function of the MetaMorph software.

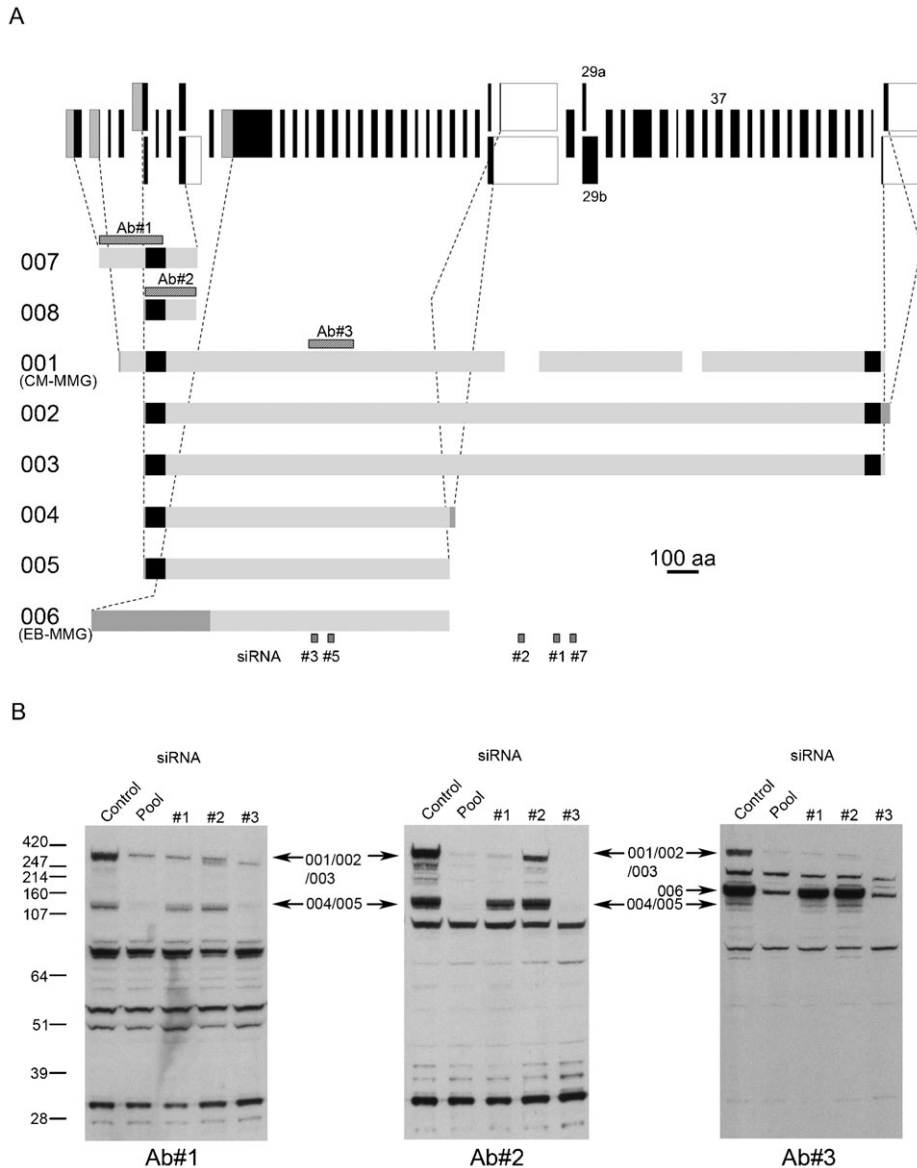


Fig. 1. The human *Myomegalin* gene encodes various isoforms. (A) The *Myomegalin* gene is composed of at least 55 exons depicted as boxes. The 5' and 3' untranslated regions of exons are shown in gray and white, respectively. According to the Ensembl database, the alternative use of exons produces at least 8 protein isoforms depicted below the gene. Gaps in the representation of isoform 1 result from the use of alternative exon 29a and lack of exon 37 use. Dotted lines show the correspondence between initiating or terminating exons and the N and C-termini, respectively. The various isoforms are encoded by a first exon (gray/black), all the following full black exons, and a last exon (black/white). The two black boxes on isoforms at the N and C-termini depict the conserved CM1 and CM2 domains, respectively. As shown, the N-terminus of isoform 6 is encoded by a single specific exon. The positions of peptides used for antibody production and of sequences corresponding to siRNA are indicated. (B) Various *Myomegalin* isoforms are expressed in RPE1 cells. RPE1 cells were treated for 48 hours with the indicated siRNA and subsequently lysed in 1% Igepal-CA630-containing buffer. 50 μ g of proteins from the lysates were separated by SDS-PAGE 4–12%, transferred onto nitrocellulose and immunoblotted with anti-*Myomegalin* antibodies Ab#1, Ab#2 or Ab#3. Bands indicated by arrows are identified according to their size and sensitivity to siRNA treatment.

Cell migration assays

3×10^4 RPE1 cells were cultivated in 6 well plates and treated with appropriate siRNA as usual. The day before filming, cells were split in 6 well plates coated with collagen (25 μ g/ml in 0.2% acetic acid) to be able to film individual cells. Phase contrast images were acquired every 2 minutes on a Zeiss Axiovert 200 microscope equipped with a thermocontrolled chamber with a $10 \times / 0.30$ Zeiss objective for 4 hours. The velocity, the distance from start to end point – as a straight line – (D) and the total track distance (T) were measured in Image J with the manual tracking plugin. Directionality was calculated as the ratio D/T. Statistical analysis of the results was done with the GraphPad Prism software.

Immunoprecipitation

Myc and/or GFP-tagged constructs were transfected in RPE1 cells. Twenty four hours later, cells were washed in PBS and lysed in 1 ml of buffer containing 20 mM TRIS, 2 mM EDTA, 150 mM NaCl, 1% NP40 and a complete protease inhibitor cocktail (Roche). Lysates were collected, incubated on ice for 15 minutes and centrifuged for 30 minutes at 4°C at 13,000 g. Fifty μ l were saved as input material. 10 μ l anti-Myc conjugated sepharose beads (Santa Cruz Biotechnology) or anti-GFP conjugated sepharose beads (Abcam) were incubated for 2 hours at 4°C. Control immunoprecipitation was performed with lysates of untransfected cells. Beads were washed 3 times in lysis buffer, suspended in Laemmli sample buffer and boiled. Samples were electrophoresed on NuPAGE Novex Bis-Tris minigels (Life Technologies) and proteins were detected by Western blot.

Results

Identification of *Myomegalin* isoforms expressed in RPE1 cells

The human *Myomegalin* gene (*PDE4DIP*) encompasses 224 kb on chromosome 1q12. In the Ensembl database it is predicted to encode 24 isoforms, 8 of which have a strong support from transcript sequences. These 8 isoforms originate from the use of common and alternative exons, leading to proteins with differences in their N-terminus, C-terminus and internal sequences (Fig. 1A). Seven of these isoforms have a conserved CM1 domain at their N-terminus, known to bind γ -TuRC (Choi et al., 2010). The three longer isoforms have a conserved CM2 domain at their C-terminus, characterized as a centrosome/Golgi targeting motif in CDK5RAP2 (Wang et al., 2010).

We first analyzed which isoforms are expressed in RPE1 cells using three different antibodies, and three siRNAs (Fig. 1B). Of the four major protein bands detected by Ab#2, two were consistent in apparent MW with isoforms 001/002/003 above 247 kDa and 004/005 around 120 kDa. The inhibitory effects of

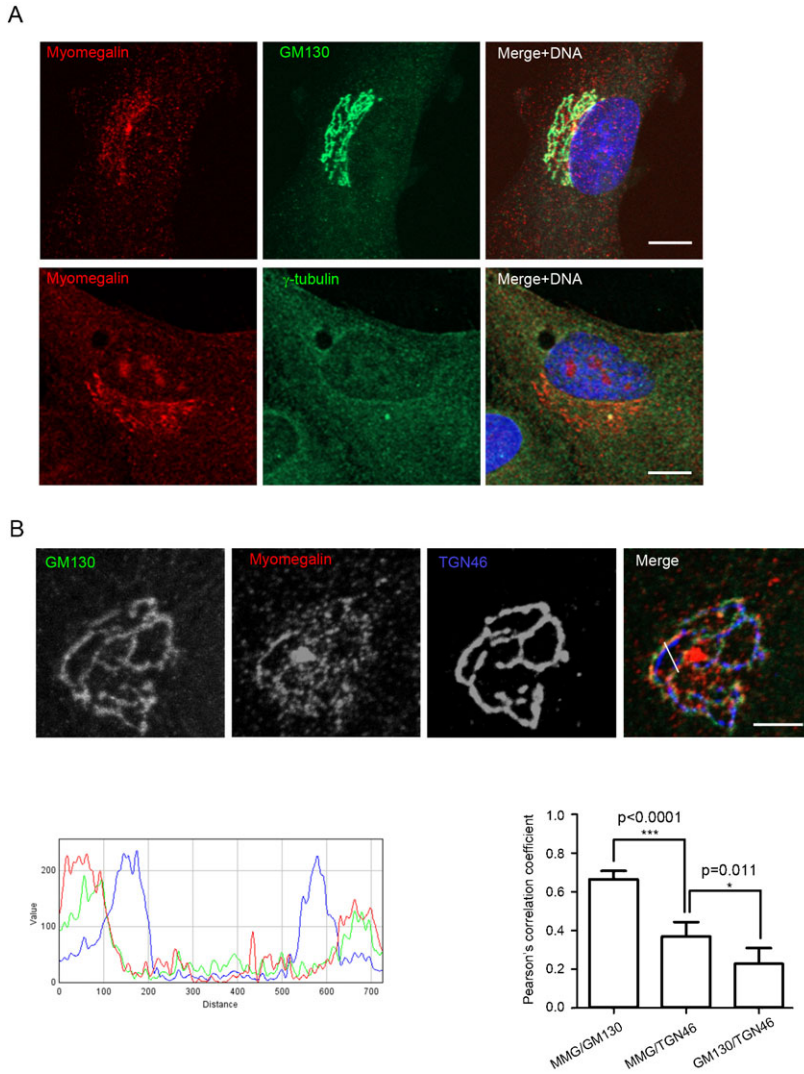


Fig. 2. Localization of Myomegalin at the centrosome and GA. (A) Resting RPE1 cells were fixed in cold methanol and stained with rabbit anti-Myomegalin Ab#1 (Red) and mouse anti-GM130 (Green) (Upper panel) or mouse anti- γ -tubulin (Green) (Lower panel). DNA was stained with DAPI (Blue). Bars, 10 μ m. (B) RPE1 cells were stained with mouse anti-GM130 (Green), rabbit anti-Myomegalin (Red) and sheep anti-TGN46 (Blue) (Upper images; bar, 5 μ m). A representative fluorescence density profile of the section indicated on the merge image is shown (Lower left). Pearson's correlation coefficients were calculated from triple labeling experiments. Values are the means \pm s.d. of 36 measures (6 measures performed at random positions in 6 different cells) (Lower right).

pooled or single siRNA confirmed this prediction, as only siRNA#3 inhibited the expression of the \sim 120 kDa isoforms, while all 3 siRNA inhibited the large ones. Two other major bands around 80 and 30 kDa were also observed; they do not correspond to predicted isoforms, and were not inhibited by siRNA, possibly reflecting non-specific antibody reactivity.

As expected, Ab#3 detected protein products corresponding to the same large (above 240 kDa) and \sim 120 kDa isoforms, albeit with a lower sensitivity than Ab#2. This lower sensitivity may account for the absence of residual large isoform in cells treated with siRNA#2, as seen with Ab#2. Interestingly, Ab#3 recognized a unique 140 kDa isoform not detected by Ab#2, and only inhibited by siRNA#3, which likely corresponds to isoform 006. This isoform lacks a CM1-containing N-terminus and has a unique C-terminus encoded by a unique alternative exon. A minor band corresponding to a protein product of 70 kDa is likely to be nonspecific for the same reasons as mentioned above for Ab#2. Ab#1 detected high molecular weight proteins very similar to Ab#2. Bands detected below 107 kDa are likely to be nonspecific as they do not correspond to any predicted Myomegalin products and are not inhibited by siRNAs.

RPE1 therefore express a complex pattern of different isoforms, which probably exert different functions within the cell.

Myomegalin localizes to the centrosome and *cis*-side of the GA. We determined the subcellular localization of Myomegalin in RPE1 cells by IF. Ab#2 and Ab#3 antibodies were not used in these experiments because i) Ab#2 showed weak cross-reactivity with the human Myomegalin paralog CDK5RAP2 at the centrosome and ii) Ab#3 gave a strong centrosomal and cytoplasmic staining that was not specific as it was not inhibited by any Myomegalin-specific siRNA either used alone or pooled. A rabbit polyclonal antibody (Ab#1) raised against a CM1-containing fragment was the most reliable and specific reagent for IF experiments. Immunostaining with this antibody indicated that Myomegalin localizes at the centrosome, the GA and punctually in the cytoplasm (Fig. 2A). A similar staining has been described in Cos-7 cells and in FRTL-5 thyroid cells (Verde et al., 2001). However, we noticed that the GA staining in RPE1 cells was present in only 20 to 30% of proliferating cells as compared to 70 to 80% of resting cells. Consequently, subsequent experiments were done with overnight serum-starved cells. In these conditions, we observed that siRNA#1 and siRNA#3 were the most efficient at inhibiting Myomegalin expression at the GA but did not induce complete depletion at the centrosome (data not shown). The decrease in Myomegalin-specific staining by

siRNA#2 was weak, as expected from Western blot experiments (data not shown; Fig. 1B). However, pooled siRNA (#1+#3) showed the strongest inhibitory effect and were used in subsequent experiments (supplementary material Fig. S1A,B). Of note, the GA showed enlargement and partial fragmentation upon Myomegalin depletion (supplementary material Fig. S1B). The IF results obtained with Ab#1 were confirmed with Ab#2, with the exception of a stronger centrosome staining probably due to the weak cross reactivity of the antibody with CDK5RAP2 (data not shown).

Our results show that RPE1 cells express CM1-containing isoforms of Myomegalin at the GA and centrosomes. However, the localization of endogenous isoform 006 was not addressed in these experiments as it is not recognized by Ab#1.

To more precisely determine Myomegalin localization at the GA, RPE1 cells were labeled with anti-Myomegalin antibody together with antibodies directed against GM130/golgin95/GOLGA2 and TGN46/TGOLN2 to label the *cis*- and *trans*-regions of the GA, respectively. We observed an extensive colocalization of Myomegalin with GM130 at the *cis*-Golgi cisternae (Fig. 2B). TGN46-labeled structures were close but distinct from anti-Myomegalin staining (Fig. 2B).

We next studied the fate of Myomegalin during GA fragmentation. First, we examined the effect of a treatment with BFA or nocodazole. These drugs disrupt the structural integrity of the GA. They respectively block the traffic from the ER to the GA and depolymerize MTs, and cause Golgi fragmentation into small punctate remnants. After 30 minutes of BFA or 3 hours of nocodazole treatment, Myomegalin was found associated with GA remnants distributed throughout the cytoplasm, indicating that the localization of Myomegalin to the GA is independent of the integrity of this organelle. Like in intact GA, the *cis*-Golgi marker GM130 showed partial colocalization with Myomegalin (supplementary material Fig. S2A). Because nocodazole depolymerizes MTs, this result further indicated that Myomegalin is associated to the GA in a MT-independent manner. Second, we followed the fate of Myomegalin in cells overexpressing the p50 subunit of dynein to inhibit dynein function, which causes fragmentation of the GA (Corthésy-Theulaz et al., 1992). Myomegalin association to GA ministacks persisted upon dynein inhibition (supplementary material Fig. S2A). Myomegalin thus localizes to the *cis*-Golgi independently of MTs and Golgi structure.

The human Myomegalin paralog CDK5RAP2 localizes to the GA in an AKAP450-dependent manner (Wang et al., 2010). Similarly, we could show that Myomegalin colocalizes with AKAP450 and depends on this protein for GA localization (supplementary material Fig. S2B,C). Interestingly, Myomegalin depletion altered localization of AKAP450 at the GA, which showed a more diffuse staining pattern in the cytoplasm and an impaired colocalization with GM130 compared to control cells. Myomegalin may thus control to some extent AKAP450 localization and/or stability (supplementary material Fig. S2D). As expected from the dependence of AKAP450 on GM130 for its presence at the GA (Rivero et al., 2009), GM130 depletion also prevented localization of Myomegalin on this organelle (supplementary material Fig. S3).

To better determine which isoforms are present at the GA and centrosome, we expressed full length and truncated GFP-tagged isoforms. We concentrated on isoforms 001 and 006 as representatives of two strikingly different forms of

Myomegalin. We named isoform 001 CM-MMG because it has a CM1 and a CM2 domains and isoform 006 EB-MMG because, as detailed below, it has a unique tandem of putative EB1 binding motifs (Fig. 3A). At low expression levels, the two full length isoforms localized at the GA in close association with the *cis*-Golgi protein GM130 (Fig. 3B), but of the two only the CM-MMG isoform was detected at the centrosome. Both N and C-terminal CM-MMG truncated proteins localized at the centrosome but only the C-terminal part of CM-MMG localized at the GA. Strikingly, EB-MMG was addressed to the GA through its N-terminus, indicating that the two isoforms have two different, non-overlapping, Golgi-targeting regions (Fig. 3B,C).

Myomegalin is involved in MT nucleation from the centrosome and GA

CM-MMG associates with γ -TuRC components

Human CDK5RAP2 and Myomegalin orthologs in various species, like *Drosophila* centrosomin, are known to associate with and to anchor γ -TuRCs MT nucleating complexes (Fong et al., 2008; Sawin et al., 2004; Zhang and Megraw, 2007). More importantly, the conserved CM1 domain not only binds γ -TuRCs directly but also stimulates its MT nucleation activity (Choi et al., 2010).

When overexpressed in RPE1 cells, four out of the six MMG constructs formed dense aggregates. In IF, aggregates formed by CM-MMG or its N-terminal part (CM-MMG_N), which has the CM1 domain, strongly recruited the γ -TuRCs components γ -tubulin (Fig. 4A), GCP2 (supplementary material Fig. S4B) and the associated protein NEDD1 (supplementary material Fig. S4A). In contrast, aggregates formed by EB-MMG_N, which is devoid of the CM1 domain, did not recruit γ -TuRCs (Fig. 4A). However, it was unique in its capacity to concentrate pericentrin (supplementary material Fig. S4C). The CM-containing Myomegalin isoforms are thus likely to bind γ -TuRCs through their CM1 domain, like other members of the same family. Surprisingly, we could not demonstrate specific binding between γ -tubulin and CM-MMG or CM-MMG_N. However, we found that a CM1-containing fragment, but not a fragment lacking the C-terminus of CM1 (Fig. 3A, CM1 and CM1 Δ C), specifically associated with endogenous and ectopic GFP-tagged γ -tubulin (Fig. 4B).

Next, we asked whether the aggregates of CM-MMG and CM-MMG_N associated with γ -TuRCs possess MT nucleation capacity. When we depolymerized MTs in transfected cells and subsequently allowed them to regrow, MT asters formed around nearly all CM-MMG and CM-MMG_N, but not control CM-MMG_C, aggregates (Fig. 5A). Strikingly, we observed that many CM-MMG_N associated asters also colocalized with anti-GM130 labeled GA remnants (Fig. 5B), suggesting that Myomegalin may participate in the regulation of MT production from the GA.

Myomegalin participates in MT nucleation from the centrosome and GA

To test our hypothesis that Myomegalin regulates MT growth from the GA and/or the centrosome, MTs were depolymerized and allowed to regrow for various lengths of time in control and Myomegalin siRNA-treated RPE1 cells. α -tubulin staining after 1 minute of regrowth revealed numerous non-centrosomal MTs in addition to the centrosomal asters in control cells. These non-centrosomal MTs were associated with the dispersed Golgi

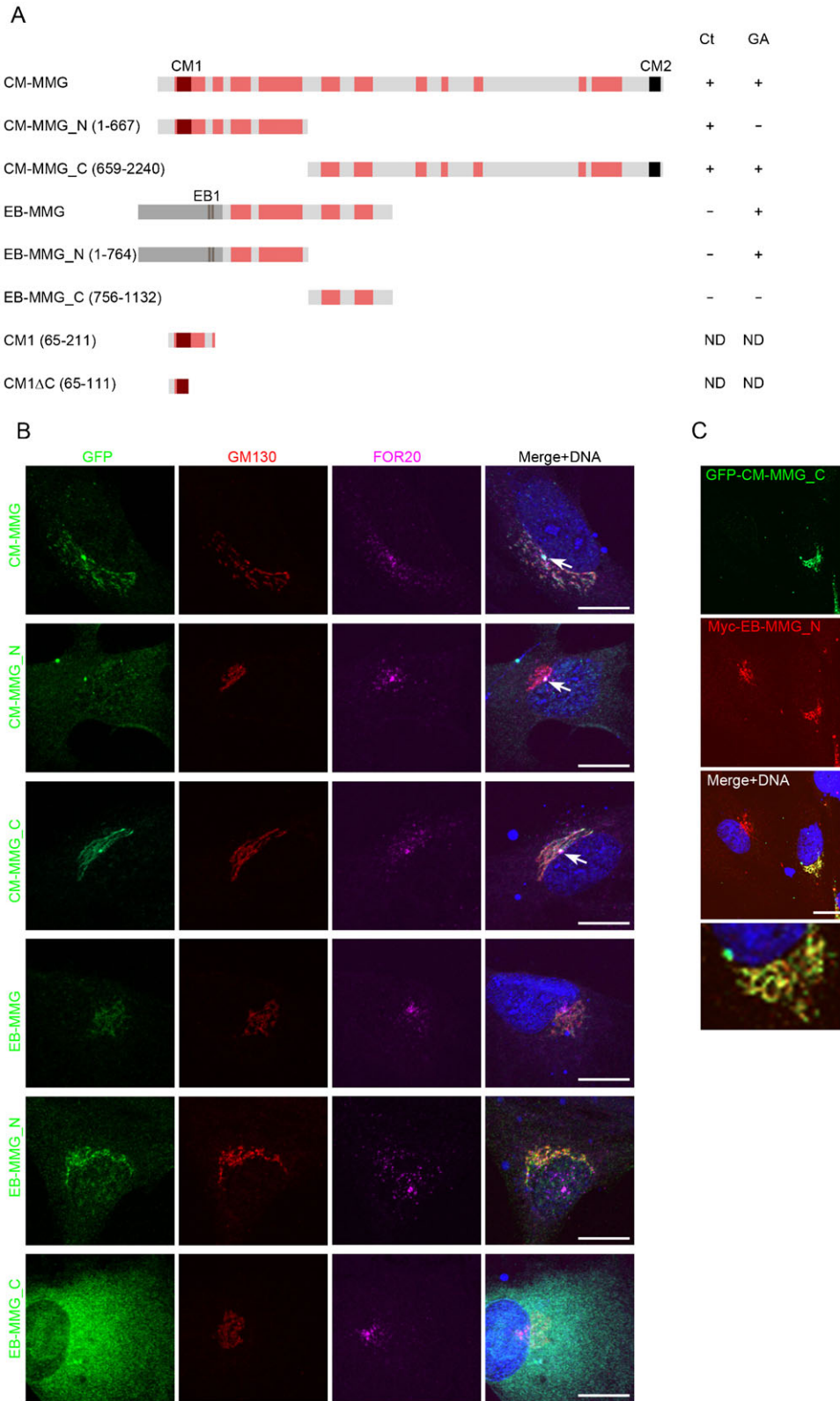


Fig. 3. Different regions are required to address the CM-MMG and EB-MMG isoforms to the GA and/or centrosome. (A) Schematic representation of the two Myomegalin isoforms and truncated proteins used in our study. Red boxes indicate coiled-coil regions and the unique sequence at the N-terminus of EB-MMG is shown in heavy gray, encompassing two putative EB1 binding motifs. A recapitulation of the localization experiments shown in panel B is presented on the right (Ct, centrosome). (B) The various GFP-tagged constructs were transfected in RPE1 cells. Cells were fixed by cold methanol at 24 hours post-transfection and labeled with mouse anti-GFP antibody (Green), rabbit anti-GM130 (Red) and rat-anti-FOR20 (Magenta) antibodies to label the *cis*-Golgi and centrosome, respectively. Centrosomes are indicated by arrows when colocalization is observed. Bars, 10 μ m. (C) RPE1 cells were transfected with expression vectors coding for GFP-tagged CM-MMG_C and Myc-tagged EB-MMG_N. Cells were fixed and labeled with mouse anti-GFP (Green) and rabbit anti-Myc (Red) antibodies. DNA was stained with DAPI. Images show a single (left) and double (right) transfected cell. At the bottom is a magnification of the GA region of the double-transfected cell. Bar, 10 μ m.

remnants, as already described (Efimov et al., 2007; Rivero et al., 2009), to which Myomegalin was associated (Fig. 6A). Myomegalin siRNA-treated cells showed a striking difference with control cells in the formation of centrosomal and non-centrosomal MTs (Fig. 6B). After 1 minute regrowth, the aster

size of Myomegalin siRNA-treated cells was diminished at the centrosome ($1.35 \pm 0.39 \mu\text{m}$ versus $0.65 \pm 0.20 \mu\text{m}$ for control and Myomegalin siRNA, respectively) (Fig. 6C) and almost totally abrogated at the Golgi remnants. After 5 minutes, the difference at the centrosome was even higher with

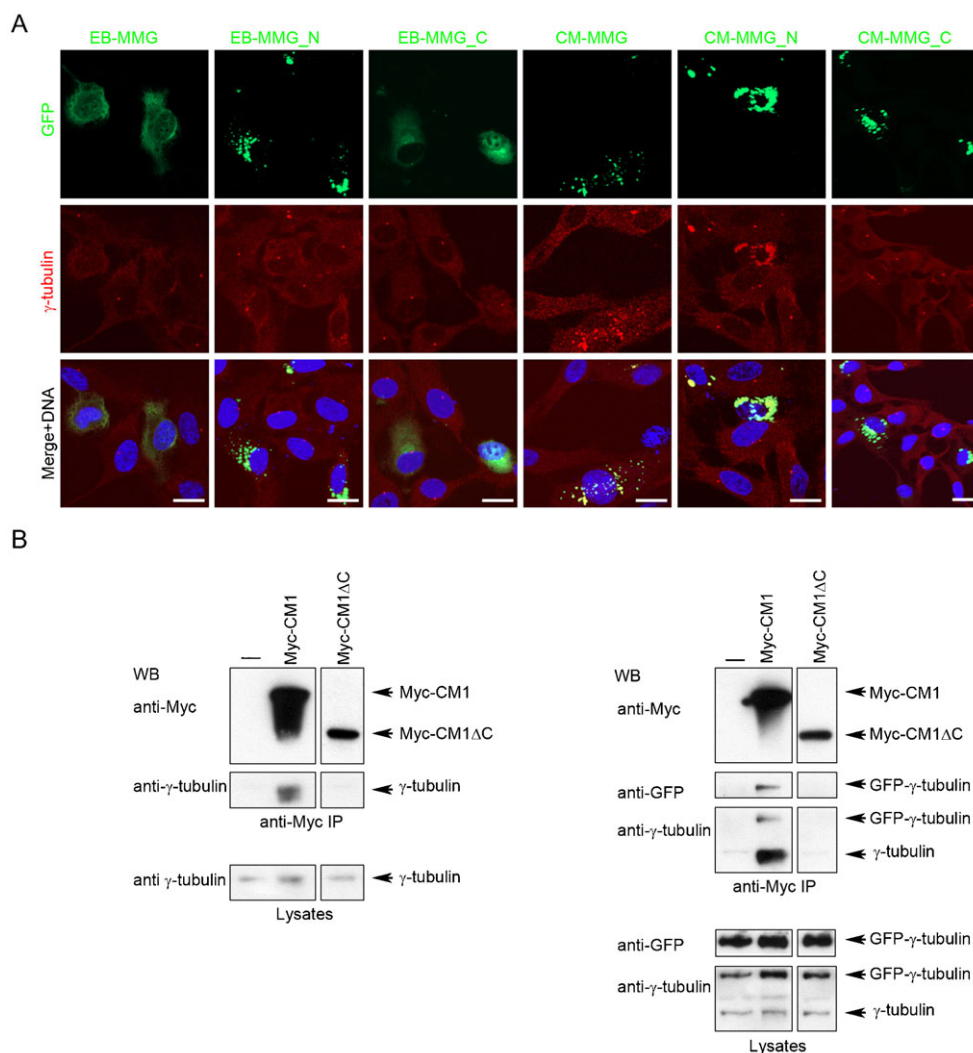


Fig. 4. CM-MMG and γ -tubulin.

(A) Asynchronous RPE1 cells were transfected with GFP-tagged wild-type and truncated Myomegalin EB-MMG and CM-MMG coding constructs and fixed in cold methanol 24 hours post transfection. Cells were labeled with mouse anti-GFP (Green) and rabbit anti- γ -tubulin (Red). DNA was stained with DAPI (Blue). Bars, 10 μ m.

(B) RPE1 cells (Left panel) or RPE1 cells stably expressing GFP- γ -tubulin (Right panel) were transfected to express the Myc-tagged CM1 and CM1 Δ C constructs (Fig. 3A). Cells were lysed 24 hours post-transfection and tagged proteins were precipitated with anti-Myc conjugated agarose beads. Immunoprecipitates were separated by SDS-PAGE, transferred onto nitrocellulose and immunoblotted with the indicated antibodies.

$7.85 \pm 2.60 \mu\text{m}$ and $1.61 \pm 0.71 \mu\text{m}$ for control and Myomegalin siRNA, respectively (Fig. 6C). However, a seemingly normal array of cytoplasmic MTs was recovered at later time points. Thus, MT regrowth is delayed in the absence of Myomegalin.

EB-MMG binds EB1 and regulates MTs

The unique sequence found at the N-terminus of Myomegalin isoform 006/EB-MMG is conserved in vertebrates. It is encoded by a single exon and does not show predicted domains. However, examination of the human sequence revealed three putative EB-1 binding motifs SxI/LP. These motifs are known to bind the end binding homology (EBH) domain of EB1 in +TIP binding partners such as CLASP, APC and CDK5RAP2 (Honnappa et al., 2009) (supplementary material Fig. S5). Validated binding motifs are found within basic serine/proline rich sequence regions. Site prediction using the Eukaryotic Linear Motif (ELM) resource confirmed that the second and third motifs of the 006/EB-MMG isoform are likely to constitute EB1 binding sites. The second motif is the best conserved in different species.

We found that EB-MMG associates with EB1 by co-immunoprecipitation in a cell line expressing GFP-EB1 and transfected with Myc-tagged full length or truncated constructs of EB-MMG. As expected, only EB-MMG and EB-MMG_N, which

have the putative EB1 binding sites, but not EB-MMG_C, which does not, were able to bind EB1 (Fig. 6A). CM-MMG did not coprecipitate with EB1 (data not shown).

In RPE1 cells with moderate levels of overexpressed EB-MMG, the latter colocalized with EB1 at MT plus-ends (Fig. 7B), suggesting that EB-MMG may have a role in MT growth and dynamics. To test this hypothesis, we first analyzed the effect of overexpressing this isoform on the localization of EB1 in RPE1 cells. We observed a striking reduction of endogenous EB1 at MT plus ends in cells overexpressing EB-MMG but not CM-MMG (Fig. 7C,D; data not shown). We also looked at EB1 localization in RPE1 cells stably expressing ectopic GFP-EB1. In this cell line overexpressed EB1 labeled MTs along their entire length, as described previously by others (Askham et al., 2002; Ligon et al., 2003). Overexpressed EB-MMG strongly displaced EB1 from MTs to a diffuse cytoplasmic and nuclear localization identical to EB-MMG staining in these cells. This effect was not observed with CM-MMG (data not shown). These observations suggest that overexpressed EB-MMG may negatively regulate MT growth by trapping EB1 away from MT plus-ends. This was indeed the case in a MT regrowth assay where MT aster size was diminished by 50% in EB-MMG overexpressing cells compared to control cells (Fig. 6E). In

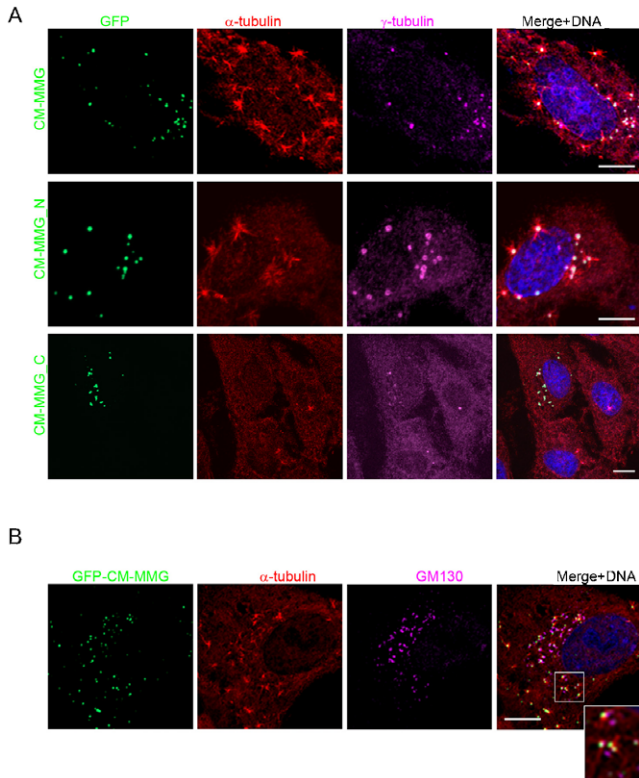


Fig. 5. CM-MMG promotes MT nucleation. (A) Asynchronous RPE1 cells were transfected with GFP-tagged wild type CM-MMG and truncated forms and cells were subjected to a MT regrowth assay 24 hours post transfection. MTs were depolymerized with a high dose of nocodazole and a cold treatment. After the drug washout and transfer to 37°C, MTs were allowed to grow for 1 minute. Cells were fixed and labeled with mouse anti- α -tubulin (Red) and rabbit anti- γ -tubulin (Magenta). DNA was stained with DAPI (Blue). Bars, 10 μ m. (B) RPE1 cells expressing GFP-CM-MMG were treated as in panel A and labeled with- α -tubulin (Red) and rabbit anti-GM130 (Magenta). The insert show a magnification of the indicated region of the merge image. Bar, 10 μ m.

addition, we used videomicroscopy to measure the velocity of GFP-EB1 comets in control and EB-MMG or CM-MMG overexpressing cells. This velocity was diminished by \sim 30% in EB-MMG but not CM-MMG cells (Fig. 7F).

Finally, Myomegalin depletion by siRNA treatment did not alter EB1 localization at MTs plus-ends. In the reverse experiment, Myomegalin still localized at the GA and centrosome when EB1 was depleted (supplementary material Fig. S6).

Migration defects in Myomegalin-depleted cells

Golgi-derived MTs are important for cell polarization and cell motility (Efimov et al., 2007; Miller et al., 2009; Nakano et al., 2010; Rivero et al., 2009). Because decreased Myomegalin expression affects MTs originating from the GA in RPE1 cells we wondered whether cell mobility was altered. We analyzed the individual movements of RPE1 cells seeded at low concentration (to prevent alteration of trajectories or speed by one cell encountering another one on its way). We tracked individual cells by time-lapse microscopy to analyze both the direction of the cell movement and the distance run by cells. We used two different siRNA pools targeting similar regions of Myomegalin mRNA, and thus likely to target the same Myomegalin isoforms (Fig. 1A). Control RPE1 cells filmed for 4 hours usually moved

in a directionally persistent fashion. Cells treated with siRNA directed against Myomegalin ran shorter distances or were even immobilized, probably according to the level of the knock-down obtained with the siRNAs. The decrease in the distance run by cells was due to a reduced velocity but not to a change in migration directionality (measured by the ratio of the distance between start and finish point divided by the total track distance) (Fig. 8A,B). Values are probably underestimated as RNAi efficiency is not absolute (especially for the #1+#3 siRNA pool).

In conclusion, Myomegalin depletion affected cell motility but not migration directionality, which suggests that cell polarization was not affected. This is reminiscent of the role of AKAP450 in migration (Rivero et al., 2009). We propose that reduced MT polymerization (by reduction of MT nucleation and/or loss of EB1 from MT +ends) is responsible for the slower migration in cells with reduced Myomegalin expression.

Discussion

Myomegalin exists as several isoforms

The consensus coding sequences (CCDS) project has identified eight CCDS in the human *Myomegalin/PDE4DIP* gene, which are consistently annotated and of high quality. Most protein variability is found at the N and C-terminus. In both cases, a specific transcript is likely to be obtained from the initiation or termination of transcription downstream of alternative promoters and polyadenylation sites, respectively. Four putative promoters and three polyadenylation sites may thus account for part of the isoform diversity. Further complexity stems from alternative splicing events, such as those regulating the use of exons 29 and 37. Our study shows that a subset of the isoforms encoded by these CCDS is expressed in RPE1 cells. Centrosomin, the *Drosophila* ortholog of Myomegalin, acts during oogenesis and embryogenesis as a complex mix of isoforms to allow centrosome function (Eisman et al., 2009). We found centrosomin isoforms related to human CM-MMG (i.e. possessing a CM1 domain at their N-terminus) but none related to EB-MMG. Different isoforms can be present in a single cell or can be differentially regulated among various tissues or developmental stages to exert different functions (Bourdon et al., 2005; Pan et al., 2008; Wang et al., 2008). At least three Myomegalin isoforms are expressed in RPE1 cells, indicating that their functions are not exclusive but that they work together in independent or coordinated cellular processes, as we discuss below. There are rare cases in which two isoforms produced from one gene display alternative sequences at a similar location in the protein, conferring two different properties or function. Such exon switching is observed for example in the *FGFR2* and *calcitonin/CRGP* genes, allowing the production of receptors binding different ligands and two different tissue-specific hormones sharing their N-terminus, respectively (Rosenfeld et al., 1983; Yan et al., 1993). The two different N-termini of Myomegalin (possessing or not a CM1 domain) confer to the protein the capacity to bind either γ -TuRCs (with CM1) or EB1 (without CM1). However, the mechanism responsible for the production of Myomegalin isoforms with or without a CM1 domain at the N-terminus does not involve alternative splicing but rather alternative promoters. Myomegalin orthologs from other species and vertebrate paralog CDK5RAP2 are related to the CM-MMG isoform. Interestingly, all vertebrate species have a *Myomegalin* gene that encodes the two isoforms with unique N-termini. It is therefore likely that the two different functions of

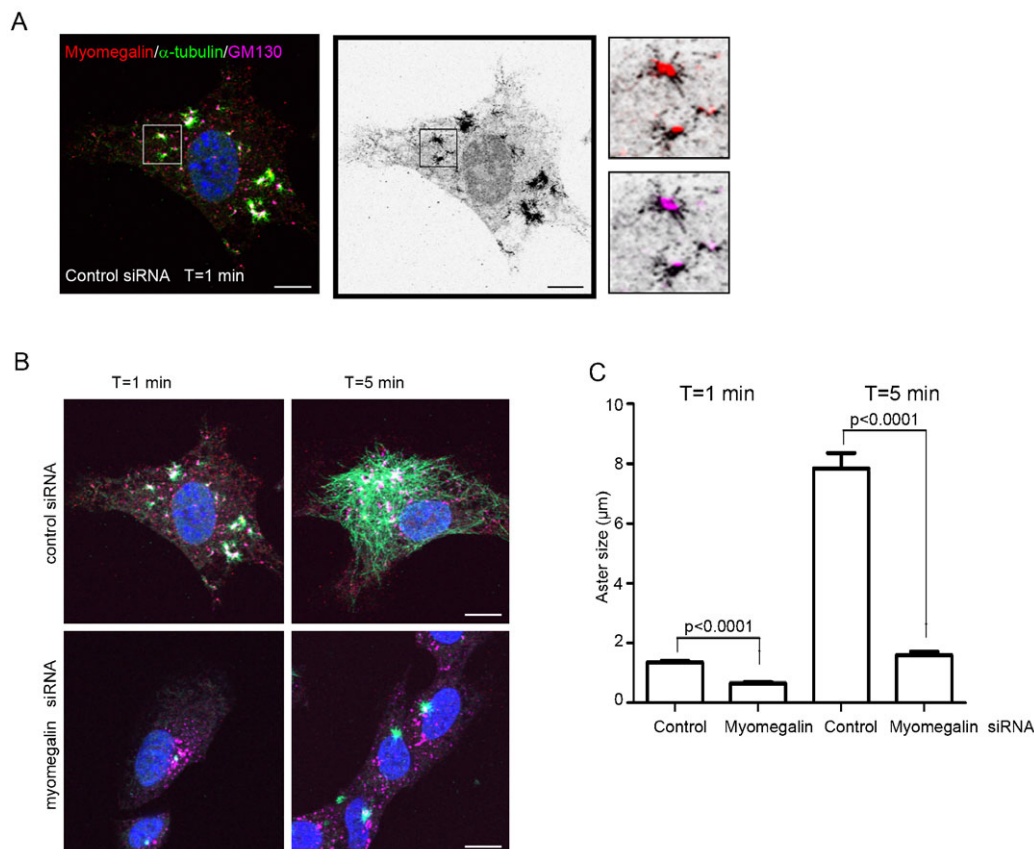


Fig. 6. Myomegalin is necessary for MT nucleation from the centrosome and GA. (A) Control siRNA-transfected RPE1 cells were starved overnight and subjected to a MT regrowth assay. MTs were depolymerized with a high dose of nocodazole and a cold treatment. After the drug washout and transfer to 37°C, MTs were allowed to grow for 1 minute. Cells were then fixed and labeled with sheep anti- α -tubulin (Green), rabbit anti-Myomegalin Ab#1 (Red) and mouse anti-GM130 (Magenta) antibodies. DNA was stained with DAPI (Blue). Tubulin labeling was converted in negative grayscale to better visualize MT asters (Middle image) and a selected region was magnified (Rightmost images) to show Myomegalin (Upper image) and GM130 (Lower image) associated with asters. Bars, 10 μ m. (B) Cells transfected with control or *Myomegalin* siRNA were treated as in panel A and MT growth was allowed for 1 and 5 minutes before fixation and staining as in panel A. Bars, 10 μ m. (C) The sizes of centrosomal asters were measured in at least 30 cells for each experimental condition. The histogram displays the mean value and bars indicate SEM. *P* values compared with the control were calculated using unpaired Student's *t*-tests.

Myomegalin, associated with the two types of isoforms, cannot work independently.

Myomegalin isoforms localize at the centrosome and GA

Myomegalin isoforms detected in RPE1 cells localize at the centrosome and the *cis*-Golgi. We found that, more specifically, the CM-MMG isoform (with conserved CM1 and CM2 domains) is present at both locations, whereas EB-MMG isoform is only detected at the *cis*-Golgi. The CM2 domain directs CDK5RAP2 to the centrosome and GA in a pericentri and/or AKAP450-dependent manner (Wang et al., 2010). The preserved localization of the CM-MMG_C truncation mutant at the two organelles is consistent with a similar role of the CM2 domain in Myomegalin. The CM-MMG_N mutant, which is not present at the GA, is consistently localized at the centrosome (Fig. 3B; data not shown). This is possibly the result of an interaction of the Myomegalin CM1 domain with γ -TuRCs anchored at the centrosome through interactions with pericentrin, AKAP450 and/or CDK5RAP2 (Fong et al., 2008; Takahashi et al., 2002). Our study also underlines the central role of AKAP450 as a scaffold to recruit proteins important for MT nucleation at the GA, such as CDK5RAP2 and Myomegalin.

Surprisingly, EB-MMG is targeted to the GA through its N-terminus, suggesting a second, CM2-independent targeting mode. The colocalization of non-overlapping CM-MMG and EB-MMG truncated forms (CM-MMG_C and EB-MMG_N) at the GA (Fig. 3C) indicates that heterodimerization is an unlikely mechanism to explain this observation. Supporting this, CM-MMG_C, but not EB-MMG_N, localizes at the centrosome.

Myomegalin regulates MTs at the centrosome and GA

We have demonstrated that inhibiting Myomegalin expression leads to decreased MT growth from the centrosome and the GA during the recovery phase following nocodazole treatment. This is consistent with the localization of Myomegalin at these two organelles (this study; Verde et al., 2001), and with the recruitment of γ -TuRCs by Myomegalin in humans and related proteins in various species (Fong et al., 2008; Sawin et al., 2004; Terada et al., 2003; Veith et al., 2005). Nucleation at a specific site relies on γ -TuRC anchoring by large scaffolding proteins such as pericentrin, AKAP450 or CEP192. Recent studies suggest that it also depends on the nucleation-activating role of Myomegalin-related proteins such as CDK5RAP2 in humans and SPC110 in budding yeast (Choi et al., 2010; Kollman et al.,

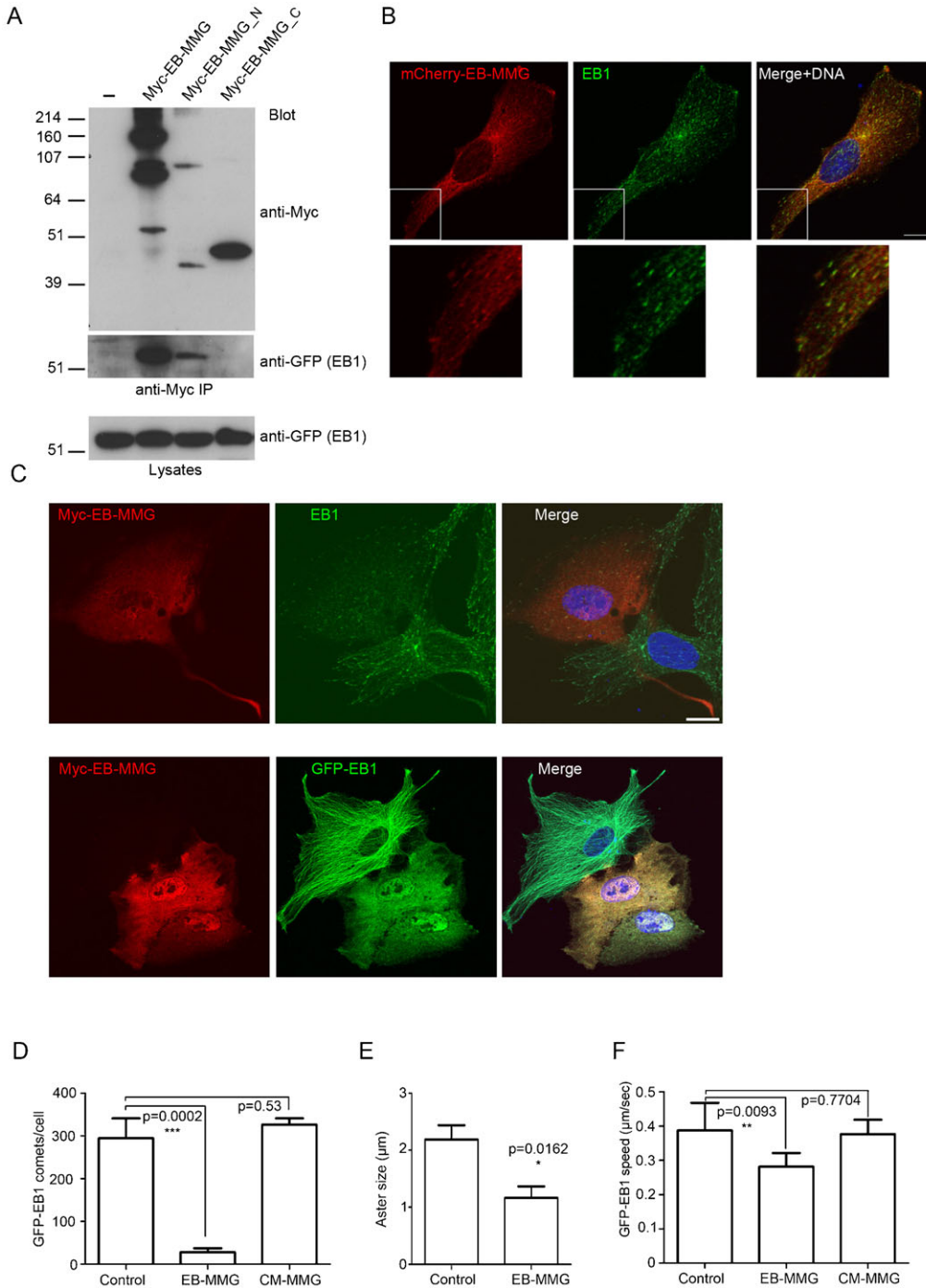


Fig. 7. EB-MMG isoform associates with EB1 and regulates MTs.

(A) RPE1 cells stably expressing GFP-EB1 were transfected to express Myc-tagged full length EB-MMG or EB-MMG N or C-terminal parts. Cells were lysed 24 hours after transfection and lysed in 1% Igepal-CA630-containing buffer. Myc-tagged proteins were isolated with anti-Myc-conjugated agarose beads. Immunoprecipitates and lysate fractions were separated by SDS-PAGE, transferred onto nitrocellulose membranes and immunoblotted with the indicated antibodies. (B) Asynchronous RPE1 cells expressing at a moderate level mCherry-EB-MMG were fixed with cold methanol 24 hours post transfection and labeled with mouse anti-EB1 (Green) and rat anti-mCherry (Red) antibodies. Magnified images of the framed region are shown to better visualize comets at MTs plus ends. Bar, 10 μm . (C) Asynchronous RPE1 cells (Upper panel) or RPE1 cells stably expressing GFP-EB1 at a high level (Lower panel) were transfected with a plasmid coding for Myc-EB-MMG and fixed with cold methanol 24 hours post transfection. Fixed cells were labeled with rabbit anti-Myc antibody (Red) and mouse anti-EB1 or mouse anti-GFP (Green) antibodies. Bar, 10 μm .

(D) The number of EB1 comets was scored in 6 different cells in each condition (i.e. in cells expressing Myc-tagged Myomegalin constructs or not). Results are represented as the mean \pm SEM. P values compared with the control were calculated using unpaired Student's t -tests. (E) We assayed MT regrowth in control and EB-MMG-overexpressing cells. The sizes of asters emanating from the centrosomes were measured at 1 minute. Results of a representative experiment out of three are shown as mean \pm SEM (Control: $n=49$, EB-MMG: $n=16$). (F) We determined the velocity of GFP-EB1 comets at the plus-ends of growing MTs in control cells and EB-MMG or CM-MMG overexpressing cells. Results are the means \pm s.d. of 60 to 160 measures performed on 11 control cells and 6 EB-MMG or CM-MMG overexpressing cells from two different experiments.

2011). Indeed, the two latter proteins are direct interactors of γ -TuRC and γ -TuSC (γ -tubulin small complex) respectively. They may help position γ -tubulin molecules at a distance compatible with tubulin protofilaments arrangement in the MT lattice (Kollman et al., 2011). Myomegalin does not seem to participate in γ -tubulin anchoring on interphase centrosomes (supplementary material Fig. S1B); it may instead play a nucleation-activating role at the centrosome and possibly at the GA. In contrast, CDK5RAP2 is required for both γ -TuRC anchoring and activation at the centrosome, because centrosomal γ -tubulin is greatly diminished following CDK5RAP2 depletion

(Fong et al., 2008). It will be of interest to determine to what extent CDK5RAP2 and Myomegalin are redundant or complementary at the centrosome. Myomegalin may also play a role similar to other centrosomal proteins such as CEP70 and Centrobin, which regulate MT elongation and/or stabilization, but are not involved in centrosomal anchoring of γ -tubulin (Lee et al., 2010; Shi et al., 2011; Shi et al., 2012).

The molecular bases of the MT organizing activity of the GA only begin to be delineated. Clearly, it requires a GM130-AKAP450- γ -TuRC complex at the *cis*-Golgi and a GCC185-CLASP complex at the *trans*-Golgi (Efimov et al., 2007; Rivero

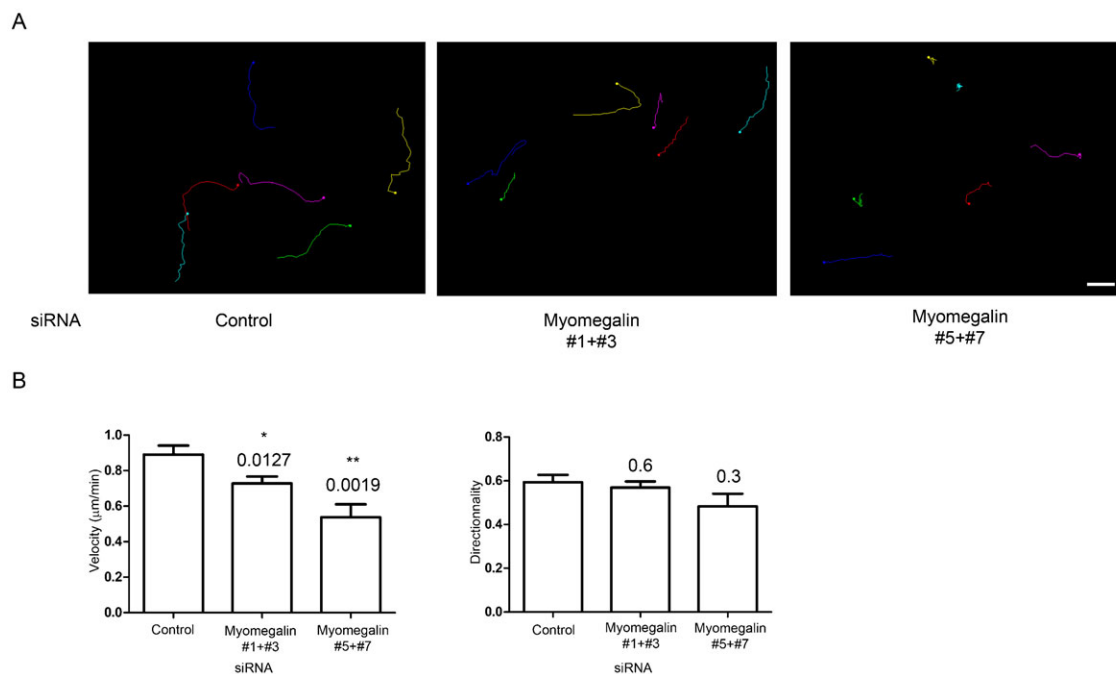


Fig. 8. Cell migration defects in Myomegalin-depleted cells. Control and Myomegalin siRNA-treated cells (treated with two different pools) were plated on collagen-coated plates and imaged every 2 minutes for 4 hours. **(A)** Representative examples of cell trajectories in each condition. Bar, 50 μm . **(B)** Migration speed of control and Myomegalin siRNA treated cells and directionality of the migration. Directionality is the ratio of direct distance from start to end point divided by the total track distance. Results of a representative experiment out of three (control: $n=17$, Myomegalin #1+#3 $n=18$, Myomegalin #5+#7 $n=19$). Histograms display the mean value and bars indicate SEM. P values compared with the control were calculated using unpaired Student's t -tests.

et al., 2009). We found that aggregates of the overexpressed CM-MMG isoform promote MT nucleation at sites associated with the *cis*-Golgi protein GM130 and AKAP450, but not pericentrin. This suggests that a GM130-AKAP450-Myomegalin- γ -TuRC complex functions in MT nucleation at the *cis*-side of the GA. CDK5RAP2 was also found at the GA and may play a redundant or complementary role together with Myomegalin (Barr et al., 2010; Wang et al., 2010). Indeed, MT nucleation was delayed but not abolished following siRNA-mediated downregulation of Myomegalin. A defect in Golgi-associated MT organization impairs Golgi polarization and directional migration in RPE1 cells (Miller et al., 2009). The defect in cell migration that we observed after inhibiting Myomegalin expression suggests that the MT cytoskeleton and/or Golgi organization is not fully functional in the absence of Myomegalin.

We found that a specific Myomegalin isoform (EB-MMG) may regulate MT growth and organization through its direct interaction with the +TIP EB1 proteins. A number of +TIP protein bind MT ends indirectly through an interaction between the EBH C-terminal domain of EB1 and an SxI/LP motif in the +TIP (Honnappa et al., 2009). EB-MMG has tandem SxLP motifs, with the N-terminal one being highly conserved in vertebrate species. The sequence context of these motifs matches the basic serine/proline-rich consensus as defined in the Eukaryotic Linear Motif (ELM) resource for a functional EB1 binding motif. Such motifs are present in MT stabilizing (CLASP, APC) and destabilizing (MCAK) +TIPs. These motifs are likely to drive the binding of EB-MMG to EB1 we observed. Interestingly the interaction of overexpressed EB-MMG with EB1 resulted in a depletion of EB1 from MT plus-ends. MT dynamics was affected, at least using GFP-EB1 velocity measurements as a readout. To what extent this

isoform was required for MT regulation in our MT regrowth assay is also not known, since we used siRNAs to downregulate most isoforms. Future experiments will require EB-MMG-specific antibodies and siRNA to confirm localization of the endogenous protein at the GA and possibly at plus-ends and to delineate its specific role in MT regulation. Similarly, we cannot exclude that depletion of the short CM1-containing isoforms 004 and 005 contributes to the phenotypes we observed. It is tempting to speculate that EB1, recruited at the GA in an EB-MMG-dependent manner, participates to the stabilization of MTs growing from the *cis*-Golgi, together with CLASP subsequently recruited at growing plus-ends at the *trans*-Golgi. EB-MMG at the Golgi surface may serve as a docking site for MTs plus-ends important for Golgi structure and/or positioning. In addition, it is possible that a cytoplasmic EB-MMG pool associates with EB1 to regulate EB1 availability or stability.

CDK5RAP2 exists as two isoforms resembling the CM-MMG isoform and also binds EB1 through an SxLP motif (Fong et al., 2009). The role of this interaction is still unclear because CDK5RAP2 inhibition only slightly affects MT dynamics and the SxLP motif in CDK5RAP2 is not conserved in all vertebrate species. We can hypothesize that in complex vertebrate organisms, MT nucleation and EB1-mediated stabilization activities must localize in very close proximity to ensure efficient and coordinated MT growth. This may be the case at the GA, but this will have to be substantiated by demonstrating the presence of EB1 (or its relative EB3) at the surface of this organelle. It is the case at the centrosome where γ -TuRC nucleation complexes are concentrated, EB1 is recruited by a CAP350-FOP complex (Yan et al., 2006). CDK5RAP2, but not Myomegalin, may recruit additional EB molecules at this site.

CDK5RAP2 alterations are associated with mitotic defects such as the formation of anastral spindles, impaired centrosomal attachment to spindle poles, abnormal mitotic spindle pole number and mitotic orientation (Barr et al., 2010; Barrera et al., 2010; Fong et al., 2008; Lizarraga et al., 2010). Mitotic Myomegalin-depleted RPE1 cells displayed normal levels of γ -tubulin, CDK5RAP2 and NEDD1 associated with spindle poles, and did not have an increased mitotic index suggestive of defects in mitosis (data not shown). CDK5RAP2 may compensate for the absence of Myomegalin in mitotic cells, but a detailed analysis of spindle structure/orientation and chromosome segregation in different cell type will be necessary to clarify the role of Myomegalin during mitosis.

In conclusion, our work establishes a role of Myomegalin in MT regulation. Future experiments are now required to clarify the specific functions exerted by the two Myomegalin isoforms at the cellular and molecular levels, and to identify the molecular complexes associated with these isoforms to perform their roles in a space and time-regulated manner. How these roles in MT regulation are integrated with the signaling activity of Myomegalin as an A-kinase anchoring and phosphodiesterase-associated protein will also be a matter of interest (Uys et al., 2011; Verde et al., 2001).

Acknowledgements

We thank A. Khodjakov for the kind gift of reagents and F. Gergely for comments on the manuscript. This work was supported by INSERM and Institut Paoli-Calmettes. F.S. was a recipient of a fellowship from the Ministère de la Recherche et de l'Enseignement Supérieur.

Competing Interests

The authors have no competing interests to declare.

References

- Akhmanova, A. and Steinmetz, M. O. (2008). Tracking the ends: a dynamic protein network controls the fate of microtubule tips. *Nat. Rev. Mol. Cell Biol.* **9**, 309-322.
- Askham, J. M., Vaughan, K. T., Goodson, H. V. and Morrison, E. E. (2002). Evidence that an interaction between EB1 and p150^{Glued} is required for the formation and maintenance of a radial microtubule array anchored at the centrosome. *Mol. Biol. Cell* **13**, 3627-3645.
- Barr, A. R., Kilmartin, J. V. and Gergely, F. (2010). CDK5RAP2 functions in centrosome to spindle pole attachment and DNA damage response. *J. Cell Biol.* **189**, 23-39.
- Barrera, J. A., Kao, L. R., Hammer, R. E., Seemann, J., Fuchs, J. L. and Megraw, T. L. (2010). CDK5RAP2 regulates centriole engagement and cohesion in mice. *Dev. Cell* **18**, 913-926.
- Bartolini, F. and Gundersen, G. G. (2006). Generation of noncentrosomal microtubule arrays. *J. Cell Sci.* **119**, 4155-4163.
- Bisel, B., Wang, Y., Wei, J. H., Xiang, Y., Tang, D., Miron-Mendoza, M., Yoshimura, S., Nakamura, N. and Seemann, J. (2008). ERK regulates Golgi and centrosome orientation towards the leading edge through GRASP65. *J. Cell Biol.* **182**, 837-843.
- Bornens, M. (2002). Centrosome composition and microtubule anchoring mechanisms. *Curr. Opin. Cell Biol.* **14**, 25-34.
- Bourdon, J. C., Fernandes, K., Murray-Zmijewski, F., Liu, G., Diot, A., Xirodimas, D. P., Saville, M. K. and Lane, D. P. (2005). p53 isoforms can regulate p53 transcriptional activity. *Genes Dev.* **19**, 2122-2137.
- Chabin-Brion, K., Marceiller, J., Perez, F., Settegrana, C., Drechou, A., Durand, G. and Poüs, C. (2001). The Golgi complex is a microtubule-organizing organelle. *Mol. Biol. Cell* **12**, 2047-2060.
- Choi, Y. K., Liu, P., Sze, S. K., Dai, C. and Qi, R. Z. (2010). CDK5RAP2 stimulates microtubule nucleation by the γ -tubulin ring complex. *J. Cell Biol.* **191**, 1089-1095.
- Corthésy-Theulaz, I., Pauloin, A. and Pfeffer, S. R. (1992). Cytoplasmic dynein participates in the centrosomal localization of the Golgi complex. *J. Cell Biol.* **118**, 1333-1345.
- Efimov, A., Kharitonov, A., Efimova, N., Loncarek, J., Miller, P. M., Andreyeva, N., Gleeson, P., Galjart, N., Maia, A. R., McLeod, I. X. et al. (2007). Asymmetric CLASP-dependent nucleation of noncentrosomal microtubules at the *trans*-Golgi network. *Dev. Cell* **12**, 917-930.
- Eisman, R. C., Phelps, M. A. and Kaufman, T. C. (2009). Centrosomin: a complex mix of long and short isoforms is required for centrosome function during early development in *Drosophila melanogaster*. *Genetics* **182**, 979-997.
- Follit, J. A., Tuft, R. A., Fogarty, K. E. and Pazour, G. J. (2006). The intraflagellar transport protein IFT20 is associated with the Golgi complex and is required for cilia assembly. *Mol. Biol. Cell* **17**, 3781-3792.
- Fong, K. W., Choi, Y. K., Rattner, J. B. and Qi, R. Z. (2008). CDK5RAP2 is a pericentriolar protein that functions in centrosomal attachment of the γ -tubulin ring complex. *Mol. Biol. Cell* **19**, 115-125.
- Fong, K. W., Hau, S. Y., Kho, Y. S., Jia, Y., He, L. and Qi, R. Z. (2009). Interaction of CDK5RAP2 with EB1 to track growing microtubule tips and to regulate microtubule dynamics. *Mol. Biol. Cell* **20**, 3660-3670.
- Honnappa, S., Gouveia, S. M., Weisbrich, A., Damberger, F. F., Bhavesh, N. S., Jawhari, H., Grigoriev, I., van Rijssel, F. J., Buey, R. M., Lawera, A. et al. (2009). An EB1-binding motif acts as a microtubule tip localization signal. *Cell* **138**, 366-376.
- Hoppeler-Lebel, A., Celati, C., Bellett, G., Mogensen, M. M., Klein-Hitpass, L., Bornens, M. and Tassin, A. M. (2007). Centrosomal CAP350 protein stabilises microtubules associated with the Golgi complex. *J. Cell Sci.* **120**, 3299-3308.
- Hurtado, L., Caballero, C., Gavilan, M. P., Cardenas, J., Bornens, M. and Rios, R. M. (2011). Disconnecting the Golgi ribbon from the centrosome prevents directional cell migration and ciliogenesis. *J. Cell Biol.* **193**, 917-933.
- Kim, H. S., Takahashi, M., Matsuo, K. and Ono, Y. (2007). Recruitment of CG-NAP to the Golgi apparatus through interaction with dynein-dynactin complex. *Genes Cells* **12**, 421-434.
- Kodani, A. and Sütterlin, C. (2008). The Golgi protein GM130 regulates centrosome morphology and function. *Mol. Biol. Cell* **19**, 745-753.
- Kodani, A., Kristensen, I., Huang, L. and Sütterlin, C. (2009). GM130-dependent control of Cdc42 activity at the Golgi regulates centrosome organization. *Mol. Biol. Cell* **20**, 1192-1200.
- Kollman, J. M., Merdes, A., Mourey, L. and Agard, D. A. (2011). Microtubule nucleation by γ -tubulin complexes. *Nat. Rev. Mol. Cell Biol.* **12**, 709-721.
- Lee, J., Jeong, Y., Jeong, S. and Rhee, K. (2010). Centrobin/NIP2 is a microtubule stabilizer whose activity is enhanced by PLK1 phosphorylation during mitosis. *J. Biol. Chem.* **285**, 25476-25484.
- Ligon, L. A., Shelly, S. S., Tokito, M. and Holzbaur, E. L. (2003). The microtubule plus-end proteins EB1 and dynactin have differential effects on microtubule polymerization. *Mol. Biol. Cell* **14**, 1405-1417.
- Lizarraga, S. B., Margossian, S. P., Harris, M. H., Campagna, D. R., Han, A. P., Blevins, S., Mudbhary, R., Barker, J. E., Walsh, C. A. and Fleming, M. D. (2010). Cdk5rap2 regulates centrosome function and chromosome segregation in neuronal progenitors. *Development* **137**, 1907-1917.
- Magdalena, J., Millard, T. H. and Machesky, L. M. (2003). Microtubule involvement in NIH 3T3 Golgi and MTOC polarity establishment. *J. Cell Sci.* **116**, 743-756.
- Marie, M., Dale, H. A., Sannerud, R. and Saraste, J. (2009). The function of the intermediate compartment in pre-Golgi trafficking involves its stable connection with the centrosome. *Mol. Biol. Cell* **20**, 4458-4470.
- Megraw, T. L., Kao, L. R. and Kaufman, T. C. (2001). Zygotic development without functional mitotic centrosomes. *Curr. Biol.* **11**, 116-120.
- Miller, P. M., Folkmann, A. W., Maia, A. R., Efimova, N., Efimov, A. and Kaverina, I. (2009). Golgi-derived CLASP-dependent microtubules control Golgi organization and polarized trafficking in motile cells. *Nat. Cell Biol.* **11**, 1069-1080.
- Nakano, A., Kato, H., Watanabe, T., Min, K. D., Yamazaki, S., Asano, Y., Seguchi, O., Higo, S., Shintani, Y., Asanuma, H. et al. (2010). AMPK controls the speed of microtubule polymerization and directional cell migration through CLIP-170 phosphorylation. *Nat. Cell Biol.* **12**, 583-590.
- Pan, Q., Shai, O., Lee, L. J., Frey, B. J. and Blencowe, B. J. (2008). Deep surveying of alternative splicing complexity in the human transcriptome by high-throughput sequencing. *Nat. Genet.* **40**, 1413-1415.
- Rivero, S., Cardenas, J., Bornens, M. and Rios, R. M. (2009). Microtubule nucleation at the cis-side of the Golgi apparatus requires AKAP450 and GM130. *EMBO J.* **28**, 1016-1028.
- Rosenfeld, M. G., Mermod, J. J., Amara, S. G., Swanson, L. W., Sawchenko, P. E., Rivier, J., Vale, W. W. and Evans, R. M. (1983). Production of a novel neuropeptide encoded by the calcitonin gene via tissue-specific RNA processing. *Nature* **304**, 129-135.
- Samejima, I., Miller, V. J., Grocock, L. M. and Sawin, K. E. (2008). Two distinct regions of Mtol are required for normal microtubule nucleation and efficient association with the γ -tubulin complex *in vivo*. *J. Cell Sci.* **121**, 3971-3980.
- Sawin, K. E., Lourenco, P. C. and Snaith, H. A. (2004). Microtubule nucleation at non-spindle pole body microtubule-organizing centers requires fission yeast centrosomin-related protein mod20p. *Curr. Biol.* **14**, 763-775.
- Shi, X., Sun, X., Liu, M., Li, D., Aneja, R. and Zhou, J. (2011). CEP70 protein interacts with γ -tubulin to localize at the centrosome and is critical for mitotic spindle assembly. *J. Biol. Chem.* **286**, 33401-33408.
- Shi, X., Wang, J., Yang, Y., Ren, Y., Zhou, J. and Li, D. (2012). Cep70 promotes microtubule assembly *in vitro* by increasing microtubule elongation. *Acta Biochim. Biophys. Sin. (Shanghai)* **44**, 450-454.
- Sütterlin, C. and Colanzi, A. (2010). The Golgi and the centrosome: building a functional partnership. *J. Cell Biol.* **188**, 621-628.
- Sütterlin, C., Polishchuk, R., Pecot, M. and Malhotra, V. (2005). The Golgi-associated protein GRASP65 regulates spindle dynamics and is essential for cell division. *Mol. Biol. Cell* **16**, 3211-3222.

- Takahashi, M., Shibata, H., Shimakawa, M., Miyamoto, M., Mukai, H. and Ono, Y.** (1999). Characterization of a novel giant scaffolding protein, CG-NAP, that anchors multiple signaling enzymes to centrosome and the golgi apparatus. *J. Biol. Chem.* **274**, 17267-17274.
- Takahashi, M., Yamagiwa, A., Nishimura, T., Mukai, H. and Ono, Y.** (2002). Centrosomal proteins CG-NAP and kendrin provide microtubule nucleation sites by anchoring γ -tubulin ring complex. *Mol. Biol. Cell* **13**, 3235-3245.
- Taskén, K. A., Collas, P., Kemmner, W. A., Witczak, O., Conti, M. and Taskén, K.** (2001). Phosphodiesterase 4D and protein kinase A type II constitute a signaling unit in the centrosomal area. *J. Biol. Chem.* **276**, 21999-22002.
- Terada, Y., Uetake, Y. and Kuriyama, R.** (2003). Interaction of Aurora-A and centrosomin at the microtubule-nucleating site in *Drosophila* and mammalian cells. *J. Cell Biol.* **162**, 757-764.
- Uys, G. M., Ramburan, A., Loos, B., Kinnear, C. J., Korkie, L. J., Mouton, J., Riedemann, J. and Moolman-Smook, J. C.** (2011). Myomegalin is a novel A-kinase anchoring protein involved in the phosphorylation of cardiac myosin binding protein C. *BMC Cell Biol.* **12**, 18.
- Veith, D., Scherr, N., Efimov, V. P. and Fischer, R.** (2005). Role of the spindle-pole-body protein ApsB and the cortex protein ApsA in microtubule organization and nuclear migration in *Aspergillus nidulans*. *J. Cell Sci.* **118**, 3705-3716.
- Venkatram, S., Tasto, J. J., Feoktistova, A., Jennings, J. L., Link, A. J. and Gould, K. L.** (2004). Identification and characterization of two novel proteins affecting fission yeast γ -tubulin complex function. *Mol. Biol. Cell* **15**, 2287-2301.
- Verde, I., Pahlke, G., Salanova, M., Zhang, G., Wang, S., Coletti, D., Onuffer, J., Jin, S. L. and Conti, M.** (2001). Myomegalin is a novel protein of the golgi/centrosome that interacts with a cyclic nucleotide phosphodiesterase. *J. Biol. Chem.* **276**, 11189-11198.
- Vinogradova, T., Paul, R., Grimaldi, A. D., Loncarek, J., Miller, P. M., Yampolsky, D., Magidson, V., Khodjakov, A., Mogilner, A. and Kaverina, I.** (2012). Concerted effort of centrosomal and Golgi-derived microtubules is required for proper Golgi complex assembly but not for maintenance. *Mol. Biol. Cell* **23**, 820-833.
- Wang, E. T., Sandberg, R., Luo, S., Khrebtkova, I., Zhang, L., Mayr, C., Kingsmore, S. F., Schroth, G. P. and Burge, C. B.** (2008). Alternative isoform regulation in human tissue transcriptomes. *Nature* **456**, 470-476.
- Wang, Z., Wu, T., Shi, L., Zhang, L., Zheng, W., Qu, J. Y., Niu, R. and Qi, R. Z.** (2010). Conserved motif of CDK5RAP2 mediates its localization to centrosomes and the Golgi complex. *J. Biol. Chem.* **285**, 22658-22665.
- Yan, G., Fukabori, Y., McBride, G., Nikolaropolous, S. and McKeehan, W. L.** (1993). Exon switching and activation of stromal and embryonic fibroblast growth factor (FGF)-FGF receptor genes in prostate epithelial cells accompany stromal independence and malignancy. *Mol. Cell. Biol.* **13**, 4513-4522.
- Yan, X., Habedanck, R. and Nigg, E. A.** (2006). A complex of two centrosomal proteins, CAP350 and FOP, cooperates with EB1 in microtubule anchoring. *Mol. Biol. Cell* **17**, 634-644.
- Zekert, N., Veith, D. and Fischer, R.** (2010). Interaction of the *Aspergillus nidulans* microtubule-organizing center (MTOC) component ApsB with gamma-tubulin and evidence for a role of a subclass of peroxisomes in the formation of septal MTOCs. *Eukaryot. Cell* **9**, 795-805.
- Zhang, J. and Megraw, T. L.** (2007). Proper recruitment of γ -tubulin and D-TACC/ Msps to embryonic *Drosophila* centrosomes requires Centrosomin Motif 1. *Mol. Biol. Cell* **18**, 4037-4049.